

Modeling the dissolution of settling CaCO_3 in the ocean

Heiko Jansen,¹ Richard E. Zeebe, and Dieter A. Wolf-Gladrow

Alfred Wegener Institute for Polar and Marine Research, Bremerhaven, Germany

Received 15 March 2000; revised 21 February 2002; accepted 21 February 2002; published 29 June 2002.

[1] The production, transport, and dissolution of carbonate shells plays an important role in the global carbon cycle. For instance, these processes affect the ocean's CO_3^{2-} concentration, which, on glacial-interglacial timescales, is involved in the regulation of atmospheric pCO_2 . The saturation state of the ocean with respect to calcium carbonate suggests that any dissolution of calcium carbonate takes place not in the water column but at the seafloor. On the other hand, several authors suggest that a significant part of the dissolution takes place in the upper part of the water column. In the present paper, a simple model is presented to investigate under which circumstances dissolution of calcium carbonate in the water column may be plausible. Our analysis also includes dissolution facilitated by CO_2 release from organic carbon remineralization, which may generate a microenvironment that is undersaturated with respect to CaCO_3 . In marine snow aggregates, however, respiration-driven dissolution is shown to be insignificant due to the size and settling velocities of the aggregates. With respect to aragonite, dissolution in the water column attributable to the bulk saturation state alone is significant and may well contribute to the alkalinity maximum in the undersaturated intermediate waters of the North Pacific Ocean. The suggested large loss of calcium carbonate dissolved in the water column (60–80% of CaCO_3 production), however, cannot be explained by the mechanisms investigated here.

INDEX TERMS: 1615 Global Change: Biogeochemical processes (4805); 4806 Oceanography: Biological and Chemical: Carbon cycling; 4842 Oceanography: Biological and Chemical: Modeling; 1055 Geochemistry: Organic geochemistry; *KEYWORDS:* CaCO_3 , calcite, aragonite, modeling, water column dissolution, marine snow

1. Introduction

[2] The present paper deals with the dissolution of biogenic carbonate particles while they are settling in the water column. As calcium carbonate producing pelagic organisms such as coccolithophorids, foraminifera, and pteropods settle through the water column and accumulate on the seafloor, they may or may not dissolve, depending on the saturation state of the bulk seawater with respect to calcite or aragonite. From a geochemical viewpoint it is of interest whether dissolution can start while the particle is sinking through the water column or only after reaching the sediments. The partitioning of this process influences the timescales on which the oceanic carbonate system equilibrates and is thus relevant for, for example, glacial-interglacial transitions. Furthermore, the ratio of organic carbon to calcium carbonate reaching the seafloor influences how much carbonate is dissolved in the pore waters [Emerson and Bender, 1981]. This in turn has consequences for the ocean's uptake capacity of atmospheric CO_2 [Archer and Maier-Reimer, 1994]. Most parts of the water column are

supersaturated with respect to calcium carbonate. The time a settling particle spends in undersaturated waters before arriving at the seafloor is very short compared to the calcite dissolution timescale. Thus it is expected that the major part of carbonate dissolution takes place in the sediments. However, observations point to CaCO_3 loss in the water column. Milliman *et al.* [1999] estimate that as much as 60–80% of the produced calcium carbonate is dissolved in the upper 500–1000 m of the ocean. In this depth range, ocean waters are supersaturated with respect to both calcite and aragonite. The mechanisms underlying the proposed loss of calcium carbonate are not understood yet.

[3] Here two scenarios are investigated, which may be attributable to water column dissolution of calcium carbonate. A given particle can either sink alone and be dissolved when entering depths that are undersaturated with respect to aragonite or calcite, respectively, or, alternatively, can be contained, together with other particles and material, in an aggregate. In the latter case, respiration of organic matter may create a chemical microenvironment around the aggregate, stimulating dissolution in supersaturated waters.

[4] Section 2 of the paper outlines a simple model simulating inorganic dissolution during particle settling. A sensitivity analysis is given to provide insight into critical parameters, and the model is applied to oceanic settings utilizing Geochemical Ocean Sections Study (GEOSECS) data. Section 3 considers the possibility of respiration-

¹Now at Meteorologisches Institut der Universität Hamburg, Hamburg, Germany.

driven dissolution. Literature data on settling velocities are discussed in Appendix A.

[5] Modeling work concerning water column dissolution of calcium carbonate shells is limited. *Pond et al.* [1971] formulated a model for settling foraminifera and concluded that they have the potential of being dissolved before reaching the seafloor. *Honjo* [1977] elaborates on modeling, observational, and experimental work, pointing out that no major dissolution of biogenic carbonates takes place in the water column. *Byrne et al.* [1984] model water column dissolution of aragonite in the Pacific Ocean and state that the dissolution of settling pteropod shells should be identified with alkalinity maxima as observed by *Fiadeiro* [1980].

[6] Our model covers main carbonate-producing pelagic organisms and gives constraints on the biological and physicochemical conditions favorable to water column dissolution. The first investigation of water column carbonate dissolution mediated by biological remineralization processes is presented. Several areas are identified where more experimental investigations are needed.

2. A Model of Physicochemical Dissolution

2.1. Model Description

[7] The water column carbonate dissolution model considers a biogenic particle comprised of either calcite or aragonite, settling through the water column. As the particle enters undersaturated waters, it experiences dissolution. A simple approach in one spatial dimension is followed. The chemistry of the bulk seawater is given as forcing data. The amount of calcite or aragonite dissolved at a certain depth is the only prognostic variable. Dissolution of biogenic carbonates in the water column depends on (1) the dissolution rate of each mineral phase, (2) the surface area in contact with water, (3) the residence time of the particles in undersaturated waters, and (4) the magnitude of undersaturation. Let $C(t)$ (mol) be the calcite or aragonite content at time t (days). The kinetics may be formulated as [*Archer*, 1996]

$$\begin{aligned} \frac{dC(t)}{dt} &= 0 \quad [\text{CO}_3^{2-}] \geq [\text{CO}_3^{2-}]_c \\ \frac{dC(t)}{dt} &= -\kappa \left(1 - \frac{[\text{CO}_3^{2-}]}{[\text{CO}_3^{2-}]_c} \right)^\eta C(t) [\text{CO}_3^{2-}] < [\text{CO}_3^{2-}]_c, \end{aligned} \quad (1)$$

where κ denotes the dissolution rate constant (per day) and η denotes the dissolution rate order. $[\text{CO}_3^{2-}]$ is the in situ carbonate ion concentration ($\mu\text{mol kg}^{-1}$) and $[\text{CO}_3^{2-}]_c$ is the carbonate ion concentration at saturation. An alternative rate equation for dissolution of aragonite has been proposed by *Acker et al.* [1987]:

$$\begin{aligned} \frac{dC(t)}{dt} &= 0 \quad [\text{CO}_3^{2-}] \geq [\text{CO}_3^{2-}]_c \\ \frac{dC(t)}{dt} &= -\kappa \left([\text{CO}_3^{2-}]_c - [\text{CO}_3^{2-}] \right)^\eta C(t) [\text{CO}_3^{2-}] < [\text{CO}_3^{2-}]_c, \end{aligned} \quad (2)$$

where they experimentally find values of $\kappa = 3.32 \pm 1.77 d^{-1}$ and $\eta = 1.87 \pm 0.15$. Sensitivity studies show that

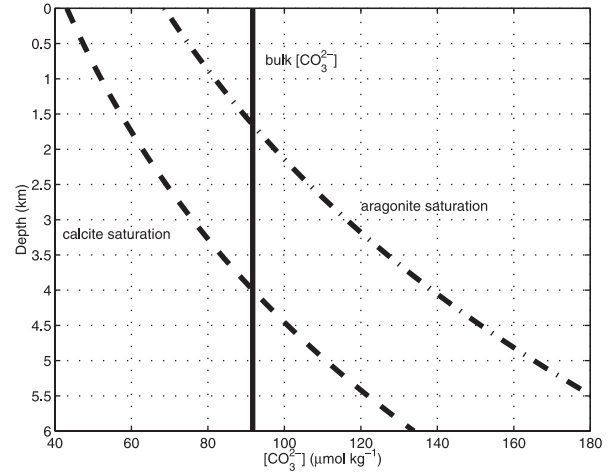


Figure 1. Critical carbonate ion concentration for calcite (dashed line) and aragonite (dash-dotted line) versus depth. Sensitivity studies are performed with bulk $[\text{CO}_3^{2-}] = 91.7 \mu\text{mol kg}^{-1} \text{CO}_3^{2-}$.

application of equation (2) versus equation (1) yields almost indistinguishable results (compare Figure 3 in section 2.2). Because an analogous formulation of equation (2) for calcite does not exist, equation (1) has been used for the modeling study presented here.

[8] The carbonate ion concentration is a function of depth (i.e., pressure; the weak dependence on temperature is neglected) and is dependent on the crystal structure, namely, calcite (foraminifera and coccolithophorids) or aragonite (pteropods):

calcite

$$[\text{CO}_3^{2-}]_c(z) = 90 \exp(0.16[z - 4])$$

aragonite

$$[\text{CO}_3^{2-}]_c(z) = 120 \exp(0.15[z - 4]), \quad (3)$$

where z is depth (km), as proposed by *Broecker and Takahashi* [1978]. Though numerically convenient because of its simplicity, this parameterization has now been seen to be unreliable [*Millero*, 1995]. Thus we have fitted equations of the form of equation (3) to critical carbonate concentrations calculated by *Millero* [1995], yielding (see Figure 1)

calcite

$$[\text{CO}_3^{2-}]_c(z) = 88.7 \exp(0.189[z - 3.82])$$

aragonite

$$[\text{CO}_3^{2-}]_c(z) = 117.5 \exp(0.176[z - 3.06]). \quad (4)$$

[9] As a first approximation, and for use in the sensitivity experiments, bulk $[\text{CO}_3^{2-}]$ is assumed to be constant and independent of depth. This is a valid simplification, as the in situ $[\text{CO}_3^{2-}]$ is virtually constant for depths >2 km, and shallower waters are generally supersaturated with respect to calcium carbonate.

Table 1. Parameters of Physicochemical Dissolution Model^a

Parameter	Standard Value	Range	Reference
η (c)	4.5	1–5	<i>Hales and Emerson</i> [1997], <i>Keir</i> [1980]
η (a)	4.2	1–5	<i>Hales and Emerson</i> [1997], <i>Keir</i> [1980]
κ (c)	5 d ⁻¹	1–7 d ⁻¹	<i>Keir</i> [1980]
κ (a)	3.2 d ⁻¹	1–7 d ⁻¹	<i>Keir</i> [1980]
ν (c, coccolithophorids)	10 m d ⁻¹	1–100 m d ⁻¹	<i>Smayda</i> [1971], <i>Fok-Pun and Komar</i> [1983]
ν (a, pteropods)	300 m d ⁻¹	80–1080 m d ⁻¹	<i>Noji et al.</i> [1997]
$[\text{CO}_3^{2-}]_{\text{bulk}}$	91.7 $\mu\text{mol kg}^{-1}$	50–250 $\mu\text{mol kg}^{-1}$	<i>Takahashi et al.</i> [1981]

^aStandard bulk concentration of CO₃²⁻ corresponds to a saturation horizon at 4 km for calcite (c) and at 2 km for aragonite (a).

[10] Let ν (m d⁻¹) be the settling velocity of the aggregate. Then, after time t the particle's depth is $z(t) = \nu t$. Thus equation (1) may be formulated as (considering calcite)

$$\frac{dC(t)}{dt} = 0 \quad t \leq t^* \quad (5)$$

$$\frac{dC(t)}{dt} = -R(t)C(t) \quad t > t^*,$$

where

$$t^* = \frac{1000 \ln([\text{CO}_3^{2-}]88.7) + 722}{0.19\nu} \quad (6)$$

is the time after which undersaturation is reached and

$$R(t) = \kappa \left(1 - \frac{[\text{CO}_3^{2-}]}{88.7} \exp[-1.9 \times 10^{-4} \nu t + 0.7] \right)^\eta \quad (7)$$

is the dissolution rate. An analogous formulation is derived for aragonite, using the appropriate parameterization in equation (4).

[11] Standard model parameters are given in Table 1. The results of the corresponding model run are shown in Figure 2. The bulk seawater concentration of 91.7 $\mu\text{mol kg}^{-1}$ CO₃²⁻ corresponds to a calcite saturation horizon at 4 km depth and an aragonite saturation horizon at 1.65 km depth. Dissolution is defined here to be visible when 1% of the particle is dissolved. In the standard model run, dissolution of calcitic shells is visible ~ 1 km below the saturation horizon. At 6 km depth, $\sim 68\%$ of a settling calcite particle is dissolved within the water column. The onset of aragonite dissolution lies ~ 1.3 km below the saturation horizon, as the pteropod shells sink faster than coccolithophorids. At 6 km depth, $\sim 57\%$ of a settling aragonite particle is dissolved within the water column.

2.2. Sensitivity Studies

[12] This section describes results obtained with sensitivity experiments. All parameters are used with standard values except the one that is varied. Sinking rates of biogenic particles determine the time the carbonate is exposed to water column dissolution. The results of numerical experiments with settling velocities varied over 2 orders of magnitude are displayed in Figure 3. Settling velocities estimated from experimental and field work are discussed in Appendix A (Tables A1 and A2). It is noted that only for sediment depths well below the saturation horizon, significant dissolution takes place in the water column provided that the settling velocity is low. The dissolution rate is

determined by the rate constant, κ , and by the order of kinetics, η , as seen in equation (1). *Keir* [1980] gives $3 \text{ d}^{-1} < \kappa < 7 \text{ d}^{-1}$ as a range for single coccoliths. The rate order of calcite dissolution kinetics is not well constrained, as values cited in the literature range from 1 [*Hales and Emerson*, 1997] to >5 [*Keir*, 1980] (compare Appendix B for a discussion on dissolution kinetics).

[13] The results of numerical experiments with dissolution rate constants $1 \text{ d}^{-1} \leq \kappa \leq 7 \text{ d}^{-1}$ are displayed in Figure 4. When compared to other parameters, varying κ has a rather minor effect on the magnitude of dissolution. Figure 5 illustrates the importance of the kinetic rate order. Varying η between 1 and 5 yields by far the largest range in model results among the sensitivity experiments. Thus

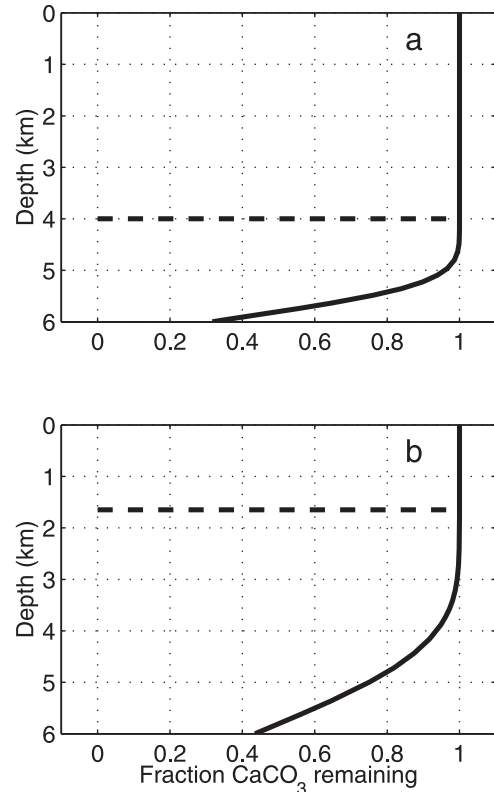


Figure 2. Model results using standard parameters as shown in Table 1 for (a) calcite and (b) aragonite shells. Shown is the fraction of calcium carbonate remaining at a certain depth. Saturation horizons are marked by straight broken lines.

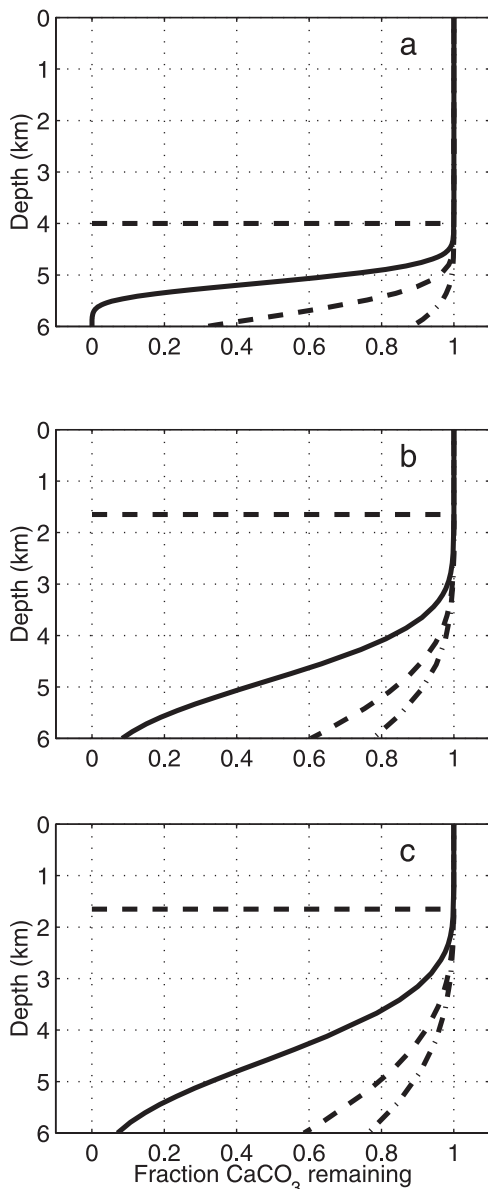


Figure 3. Influence of settling velocity on dissolution of (a) calcite and (b) aragonite particles. Shown is the fraction of calcium carbonate remaining at a certain depth. Standard parameter values are as given in Table 1. Calcite shells settle with 1 m d^{-1} (solid line), 10 m d^{-1} (dashed line), and 100 m d^{-1} (dash-dotted line), while aragonite tests sink with 100 m d^{-1} (solid line), 500 m d^{-1} (dashed line), and 1000 m d^{-1} (dash-dotted line). (c) Same as Figure 3b but with dissolution kinetics proposed by *Acker et al.* [1987] (see equation (2)).

better constraints on this parameter by experimental work are most desirable.

2.3. Application to Oceanic Settings

[14] Up to now, profiles with constant CO_3^{2-} bulk concentration have been used. In order to resolve the origin of the relatively shallow alkalinity maximum in the Pacific

Ocean [*Fiadeiro*, 1980], the model is run with the in situ profile of the CO_3^{2-} concentration in this region (Figures 6 and 7). Both the Indian Ocean and the Atlantic Ocean are too supersaturated with respect to CO_3^{2-} to yield significant inorganic carbonate dissolution in the water column. The model is applied to the specific oceanic setting with standard settling velocities (10 m d^{-1} for calcite (coccolithophorids) and 300 m d^{-1} for aragonite (pteropods)) and with various parameterizations for the dissolution kinetics proposed in the literature (Table 2).

[15] Results for the equatorial Pacific are illustrated in Figure 8. In complete analogy the North Pacific region is considered (Figure 9). In the equatorial Pacific region, between 50 and 100% of the initial calcite is dissolved at 6 km depth, depending on the kinetic parameterization. The onset of aragonite dissolution is seen $\sim 0.5 \text{ km}$ below the saturation horizon. At 6 km depth, between 55 and 96% of aragonite (pteropods) is dissolved in the water column. However, aragonite dissolution kinetics are not as thoroughly experimentally investigated as calcite dissolution kinetics, so a rate order smaller than 3 cannot be excluded, which would lead to increased amounts of aragonite dissolution in the water column.

[16] The North Pacific model run shows increased dissolution mainly for calcite: Dissolution starts close to the saturation horizon at $\sim 1.2 \text{ km}$ water depth. Between 2 and 3 km depth, dissolution slows down due to the near-equili-

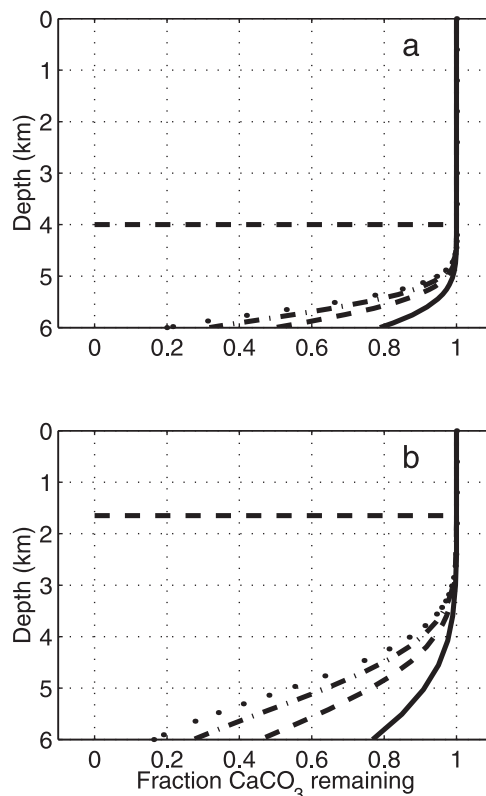


Figure 4. Influence of variations in dissolution rate constant on dissolution of (a) calcite and (b) aragonite shells. Solid line, $\kappa = 1 \text{ d}^{-1}$; dashed line, $\kappa = 3 \text{ d}^{-1}$; dash-dotted line, $\kappa = 5 \text{ d}^{-1}$; dotted line, $\kappa = 7 \text{ d}^{-1}$.

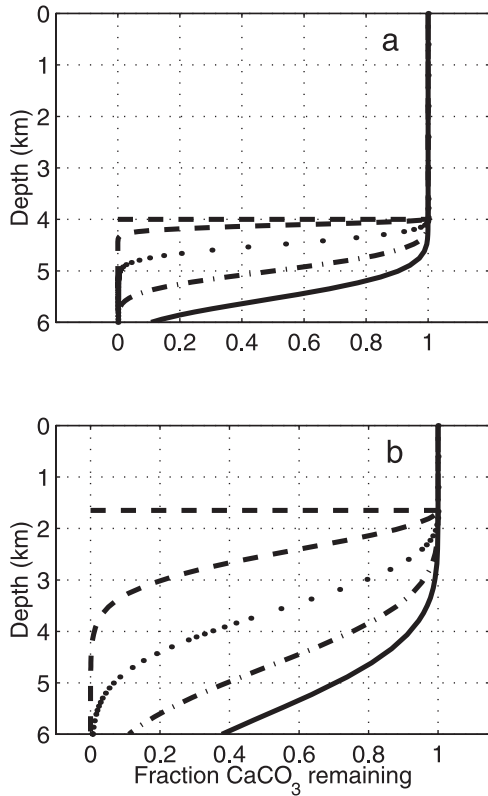


Figure 5. Influence of variations in kinetic rate order on dissolution of (a) calcite and (b) aragonite shells. Solid line on left, $\eta = 1$; dashed line, $\eta = 2$; dash-dotted line, $\eta = 3$; dotted line, $\eta = 4$; solid line on right, $\eta = 5$.

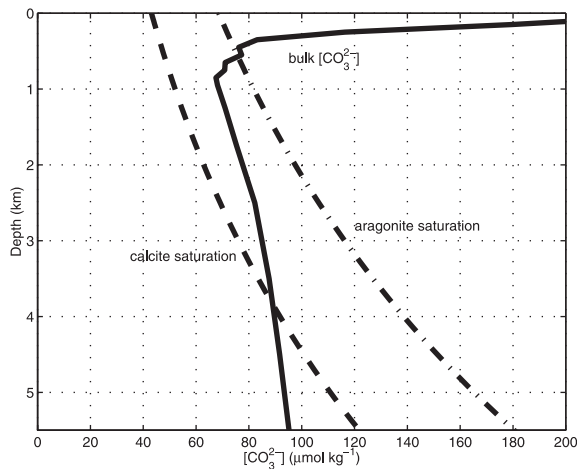


Figure 6. In situ carbonate concentration (solid line) and critical carbonate concentration in equatorial Pacific (Geochemical Ocean Sections Study (GEOSECS) data [Takahashi *et al.*, 1981]). Critical carbonate concentrations for calcite (dashed line) and aragonite (dash-dotted line) are shown. Note that saturation horizons of the two mineral phases are separated by >3 km.

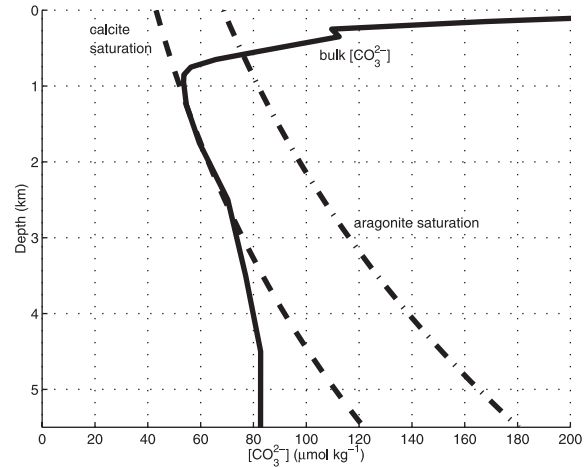


Figure 7. In situ carbonate concentration (solid line) and critical carbonate concentration in North Pacific (GEOSECS data [Takahashi *et al.*, 1981]). Critical carbonate concentrations for calcite (dashed line) and aragonite (dash-dotted line) are shown.

rium situation (Figure 7). With linear kinetics, nearly all calcite is dissolved at 4 km depth, which is at the onset of calcite dissolution in the equatorial Pacific. Aragonite dissolution reaches 100%. The parameterizations of Morse *et al.* [1979] and of Byrne *et al.* [1984] yield almost indistinguishable results.

[17] The drastic difference in calcite dissolution between the equatorial and North Pacific is due to the location of the calcite saturation horizon. As can be seen in Figures 6 and 7, the saturation horizons of calcite and aragonite are separated by ~ 3 km in the equatorial Pacific, while they are both shallower than 1 km in the North Pacific.

3. A Model of Respiration-Driven Dissolution

[18] Marine snow aggregates provide an important pathway of transport of biogenic matter from the surface to the ocean interior [Shanks and Trent, 1980; Alldredge and Silver, 1988; Alldredge and Gotschalk, 1988; Diercks and

Table 2. Parameterizations of Dissolution Kinetic According to Equation (1)

k_s, d^{-1}	η , dimensionless	Reference
<i>Calcite</i>		
5	4.5	Keir [1980]
1	2.9	Walter and Morse [1985]
5	3.0	Morse [1978]
0.38	1.0	Hales and Emerson [1997]
<i>Aragonite</i>		
3.18	4.2	Keir [1980] ^a
13.2	4.2	Keir [1980] ^b
1.1	2.93	Morse <i>et al.</i> [1979]
1.3	3.1	Byrne <i>et al.</i> [1984] ^c

^aPteropod shells.

^bSynthetic aragonite.

^cFit to model results.

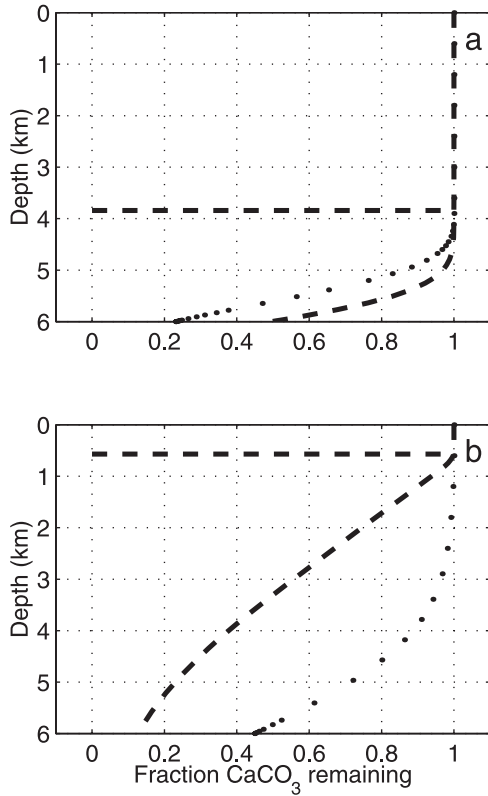


Figure 8. Dissolution of (a) calcite and (b) aragonite shells in equatorial Pacific. Parameter values are as given in Table 2. Figure 8a: solid line, $(\kappa, \eta) = (0.38, 1)$; dash-dotted line, $(\kappa, \eta) = (5, 3)$; dotted line, $(\kappa, \eta) = (1, 2.9)$; dashed line, $(\kappa, \eta) = (5, 4.5)$. Figure 8b: solid line, $(\kappa, \eta) = (1.3, 3.1)$; dash-dotted line, $(\kappa, \eta) = (13.2, 4.2)$; dotted line, $(\kappa, \eta) = (1.1, 2.93)$; dashed line, $(\kappa, \eta) = (3.18, 4.2)$.

Asper, 1997]. Phytoplankton, fecal pellets, and organic debris collide by differential settlement and collision in shear flow and stick together with a finite probability, forming macroaggregates sized up to the order of millimeters. As the organic matter inside a marine snow aggregate is respired, a microenvironment might form with locally enhanced CO_2 concentration, resulting in decreased CO_3^{2-} concentration. In this way, carbonate dissolution well above the saturation horizon might be possible. This section presents a model of a marine snow aggregate and the processes inside to estimate the effect of CO_2 respiration through organic matter remineralization on calcite dissolution.

3.1. Model Description

[19] The aggregate is modeled as an idealized porous sphere consisting of water, organic carbon, and calcite. Initial data are the C_{org} content ($\mu\text{g C}$), the calcite content ($\mu\text{g CaCO}_3$), and the porosity. The volume of the aggregate is then calculated as

$$V_a = \frac{V_c + V_{\text{cal}}}{1 - \phi}, \quad (8)$$

where ϕ is the porosity and V_c and V_{cal} (m^3) are the volumes of the organic carbon and calcite content, respectively, which

are derived from mass via the specific densities. The standard value for porosity is $\phi = 0.9$, following in situ observations by *Allredge and Gotschalk* [1988]. The settling velocity v (m d^{-1}) is calculated via the parameterization by *Allredge and Gotschalk* [1988], who observed settling velocities of marine snow aggregates to be less than those of an equivalent spherical particle settling according to Stokes' law:

$$v = 50d_a^{0.26}, \quad (9)$$

where $d_a = 2r_a$ (mm) is the diameter of the aggregate.

[20] The CO_2 produced by organic matter respiration is assumed to be released at the spherical surface of the aggregate. Dissolution via chemical alteration of the micro-environment requires the establishment of a stable diffusive boundary layer around the sinking particle, for which the aggregate radius and the sinking velocity are crucial. The concentration C_a of a dissolved species (i.e., CO_2 , CO_3^{2-} , NO_3^- , or O_2) at the aggregate surface may be calculated using the relation [*Ploug et al.*, 1999b]

$$Q = 4\pi r_a^2 D \frac{C_\infty - C_a}{\delta_{\text{eff}}}, \quad (10)$$

where Q (mol s^{-1}) is the area-integrated flux of the dissolved species in question out of the aggregate and D ($\text{m}^2 \text{s}^{-1}$) is

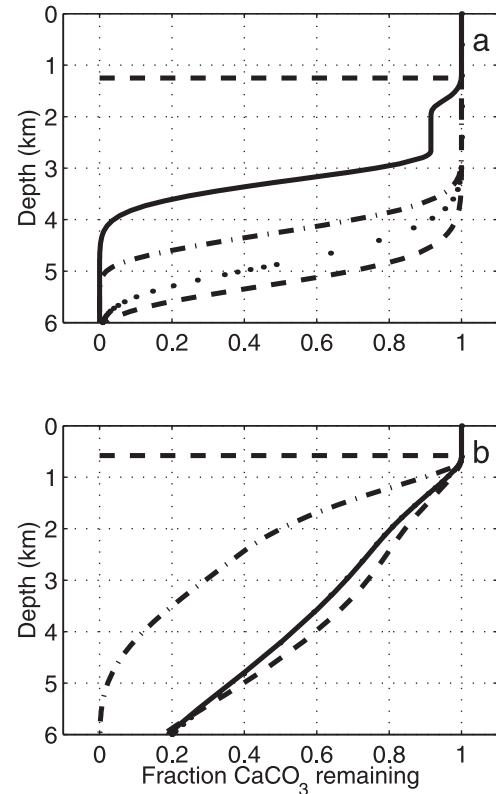


Figure 9. Dissolution of (a) calcite and (b) aragonite shells in North Pacific. Parameter values are as given in Table 2. Figure 9a: solid line, $(\kappa, \eta) = (0.38, 1)$; dash-dotted line, $(\kappa, \eta) = (5, 3)$; dotted line, $(\kappa, \eta) = (1, 2.9)$; dashed line, $(\kappa, \eta) = (5, 4.5)$. Figure 9b: solid line, $(\kappa, \eta) = (1.3, 3.1)$; dash-dotted line, $(\kappa, \eta) = (13.2, 4.2)$; dotted line, $(\kappa, \eta) = (1.1, 2.93)$; dashed line, $(\kappa, \eta) = (3.18, 4.2)$.

Table 3. Parameter Values

Symbol	Parameter	Value	Reference
ϕ	porosity	0.9	<i>Allredge and Gotschalk</i> [1988]
	C _{org} content	0–15 $\mu\text{g C}$	compare Table 4
	calcite content	0–3 μg	<i>Beers et al.</i> [1986]; <i>Tyrell and Taylor</i> [1996]
	density calcite	2.7 g cm^{-3}	<i>Young</i> [1994]
	density C _{org}	1.07 g cm^{-3}	<i>Young</i> [1994]
κ	calcite dissolution rate constant	5 d^{-1}	<i>Keir</i> [1980]
η	calcite dissolution rate order	4.5	<i>Keir</i> [1980]
λ	C _{org} decomposition time constant	1/15 d^{-1}	<i>Westrich and Berner</i> [1984]
$r_{-\text{O}_2:\text{C}}$	Redfield ratio O ₂ to C	170/117	<i>Anderson and Sarmiento</i> [1994]

the appropriate diffusion coefficient. C_∞ and C_a (mol m^{-3}) are the concentration of the species in the bulk medium and at the aggregate surface, respectively, and δ_{eff} (m) is the effective thickness of the diffusive boundary layer. Because of shear, the latter decreases with increasing settling velocity. The relative increase of advection compared to diffusivity is described by the Sherwood number Sh [*Sherwood et al.*, 1975]:

$$Sh = \frac{r_a}{\delta_{\text{eff}}}. \quad (11)$$

In a stagnant fluid, $Sh = 1$, and thus $\delta_{\text{eff}} = r_a$. The Sherwood number varies with both the Reynolds number Re and the Péclet number Pe :

$$Re = \frac{\nu r_a}{\nu} \quad (12)$$

$$Pe = \frac{\nu r_a}{D},$$

where ν is the kinematic viscosity of sea water ($\sim 0.7 \times 10^{-6} \text{ m}^2 \text{ s}^{-1}$).

[21] Parameterizations of the Sherwood number are given by *Karp-Boss et al.* [1996]:

$$Sh = 1 + 0.29(Pe)^{1/2}, \quad Re \ll 1 \quad Pe < 0.01,$$

$$Sh = 1.014 + 0.15(Pe)^{1/2}, \quad Re \ll 1 \quad 0.01 < Pe < 100, \quad (13)$$

$$Sh = 0.55(Pe)^{1/3}, \quad Re < 1, \quad Pe > 100.$$

[22] Solving equation (10) for C_a and using equation (11) yields

$$C_a = C_\infty - \frac{Q}{4 \pi r_a D Sh}. \quad (14)$$

Applying equation (14), we calculate ΣCO_2 and alkalinity concentrations at the aggregate surface, considering the fluxes deriving from remineralization of organic matter and dissolution of carbonate. From ΣCO_2 and alkalinity, $[\text{CO}_3^{2-}]$ is derived via the carbonate dissociation constants from *Department of Energy* [1994] and using pressure corrections by *Culberson and Pytkowicz* [1968].

[23] In the case of undersaturation, calcite is dissolved as described in section 2.1 (equation (1) and Table 1). Organic carbon is remineralized according to first-order kinetics,

$$\frac{dC_{\text{org}}}{dt} = -\lambda C_{\text{org}}(t), \quad (15)$$

where λ (d^{-1}) is the remineralization rate constant; that is, $1/\lambda$ gives the e-folding time. Respiration of 1 mol organic carbon consumes $r_{-\text{O}_2:\text{C}}$ moles oxygen, where $r_{-\text{O}_2:\text{C}}$ is the Redfield ratio of oxygen to carbon (compare Table 3). Using equation (14) and bulk oxygen concentrations from GEOSECS data [*Takahashi et al.*, 1981], the maximal amount of C_{org} is calculated that may be oxidized in one time step, avoiding oxygen depletion.

[24] The numerical implementation of the model is as follows. Initial conditions are the content of calcite and organic carbon. The radius of the aggregate and initial settling velocity are computed. The time step is set to 6 hours. At each time step, for each dissolved species, the Sherwood number is computed from the radius and settling velocity. Then the fluxes of CO₂ and NO₃⁻ are derived from the remineralization of organic matter. In the case of undersaturation the flux of CO₃²⁻ is calculated. From these fluxes and the bulk chemistry, ΣCO_2 and TA at the aggregate surface are derived according to equation (14), setting the new value for calcite saturation. The radius of the aggregate is decreased according to the amounts of organic matter respired and calcite dissolved, while keeping porosity constant. Then the new settling velocity and depth are computed. This scheme is iterated until the aggregate has reached the seafloor at a prescribed depth.

3.2. Parameter Values

[25] The model parameter values are given in Table 3. Experimentally derived parameterizations of the calcite dissolution kinetic are discussed in Appendix B. *Westrich and Berner* [1984] give a compilation of experimentally determined first-order decay constants for oxic organic matter decomposition. The e-folding time varies between 11 and 122 days, with a mean of 32 days. *Walsh et al.* [1988] find an average e-folding time of 38 days in sediment traps deployed in three North Pacific stations. Experimentally, *Westrich and Berner* [1984] derive e-folding times of 15 days for oxic decomposition; this value has been used for the model runs.

[26] The aggregate's calcite content is considered to be *Emiliania huxleyi* cells. In a field study of two *E. huxleyi* blooms in the Gulf of Maine, *Balch et al.* [1991] find 25–100 and 100–400 coccoliths per cell. *Fernández et al.* [1993] point out that numbers are much lower in open ocean blooms, as they find 20–40 coccoliths per cell in an *E. huxleyi* bloom in the northeast Atlantic Ocean. *Tyrell and Taylor* [1996] state that 10–50 coccoliths per cell is

Table 4. Organic Carbon Content of Marine Snow Aggregates^a

Reference	POC	Time, Location
<i>Allredge</i> [1976]	6.90	July–Aug., Gulf of California
<i>Allredge</i> [1979]	3.37	July–Aug., Gulf of California
<i>Allredge</i> [1979]	4.32	Oct.–March, Santa Barbara Channel
<i>Shanks and Trent</i> [1980]	1.36	June–July, Monterey Bay
<i>Hebel</i> [1983]	3.21	June, Point Sur
<i>Hebel</i> [1983]	1.23	June, Monterey Bay
<i>Prezelin and Allredge</i> [1983]	0.1	April, Santa Barbara Channel
<i>Prezelin and Allredge</i> [1983]	0.71	July, northeast Atlantic
<i>Allredge and Gotschalk</i> [1988]	0.4–222 ^b	March–July, San Pedro Basin, Santa Barbara Channel
<i>Allredge and Gotschalk</i> [1989]	12.3 ^b	Feb.–Sept., Santa Barbara Basin, California Current
<i>Ploug et al.</i> [1999a]	3.87–7.77	June, Catalina Island

^aParticulate organic carbon (POC) values are in $\mu\text{g C}$ per aggregate.

^bCalculated via dry weight assuming that marine snow particles are $\sim 20\%$ carbon.

typical, with one coccolith containing 1.7–8.3 μg calcite. *Trent* [1985] and *Beers et al.* [1986] observed coccolithophorid cell numbers per aggregate ranging between 180 and 870. Assuming 30 coccoliths per cell, 5 μg calcite per coccolith, and 1000 cells per aggregate yields 0.15 μg calcite ($\cong 1.8 \times 10^{-2}$ $\mu\text{g C}$). There are hints that at the end of the bloom, when marine snow aggregates are formed, the coccolithophorids are more heavily plated [*Balch et al.*, 1991]. Adopting 100 coccoliths per cell and 5000 cells per aggregate gives 2.5 μg calcite content at the upper end of the range.

[27] The organic carbon content of marine snow aggregates generally ranges from 0.1 to 12 $\mu\text{g C}$, but may be as high as 220 $\mu\text{g C}$ (Table 4). The calculations presented here adopt values of 1–15 $\mu\text{g C}$ per aggregate. It has to be stressed that there is no functional relationship between organic carbon content and the number of cells of calcareous organisms contained in a marine snow particle.

3.3. Model Runs

[28] In order to investigate the capacity of respiration-driven dissolution, a number of model runs are performed (Table 5). Figures 10 and 11 show results of a model run with GEOSECS data of the North Pacific [*Takahashi et al.*, 1981] determining the bulk carbonate system. A marine snow aggregate is considered, consisting of 15 $\mu\text{g C}_{\text{org}}$ and 1000 *E. huxleyi* cells, with 0.15 μg calcite.

[29] The initial diameter (Figure 11b) is 1.75 mm, which lies in the range of marine snow aggregates observed by *Allredge and Gotschalk* [1988]. The settling velocity is initially 58 m d^{-1} and decreases down to 42 m d^{-1} (Figure 11a). The Sherwood numbers decrease from 4–5

down to 2–3. This results in the diffusive boundary layer thickness ranging between 25 and 200 μm , which conforms to work by *Allredge and Cohen* [1987], who measured chemical boundary layers hundreds of micrometers thick in marine snow aggregates in a flow tank, simulating advective forces as they appear when the aggregate is settling through the water column. Respiration of the organic matter increases [CO₂] at the aggregate surface over the bulk concentration by a maximum of 7 $\mu\text{m kg}^{-1}$ (Figure 10a), which lowers the calcite saturation, as is visible in Figure 10c. However, because of rather fast settling velocities and slow dissolution kinetics, this does not have a significant effect on calcite dissolution. At a depth of 3 km, nearly all organic matter has been respired, so the amount of calcite dissolution at this depth is a good measure for dissolution attributable to respiration effects. Here, a mere 0.1% of the calcite content is dissolved, in contrast to no dissolution in the absence of organic matter remineralization.

[30] The model is then tested for different dissolution kinetics proposed in the literature (Table 2). As *Keir's* [1980] is the only work specifically dealing with coccoliths, it is assumed to be the most adequate kinetic for the present model. However, other results should not be excluded; for example, the work of *Walter and Morse* [1985] deals with low-Mg calcite, which is attributable to coccoliths. At 3 km depth, no calcite dissolution is evident in the equatorial Pacific, no matter what kinetic parameters are chosen. Figure 12 shows the same model run as Figure 10, but with dissolution kinetics proposed by *Morse* [1978] ($\kappa = 5 \text{ d}^{-1}$, $\eta = 3$). In this case, 4% of the initial calcite content is dissolved at 3 km depth, compared to 0.04% without organic matter remineralization.

Table 5. Initial Conditions and Parameter Settings of Model Runs

C_{org} , $\mu\text{g C}$	CaCO ₃ , μg	(κ , η), d^{-1} , dimensionless	ϕ	Ocean Basin	Results
15	0.15	(5,4.5)	0.9	North Pacific	Figures 10 and 11
15	0.15	(5,3)	0.9	North Pacific	Figure 12
0–15	0.15	varied	0.9	North Pacific	Table 6
0–15	2.5	varied	0.9	North Pacific	Table 7
5–15	1	(5,4.5)	0.1–0.9	equatorial and North Pacific	Figure 13
10	1	(5,4.5)	0.3	North Pacific	Figures 14 and 15

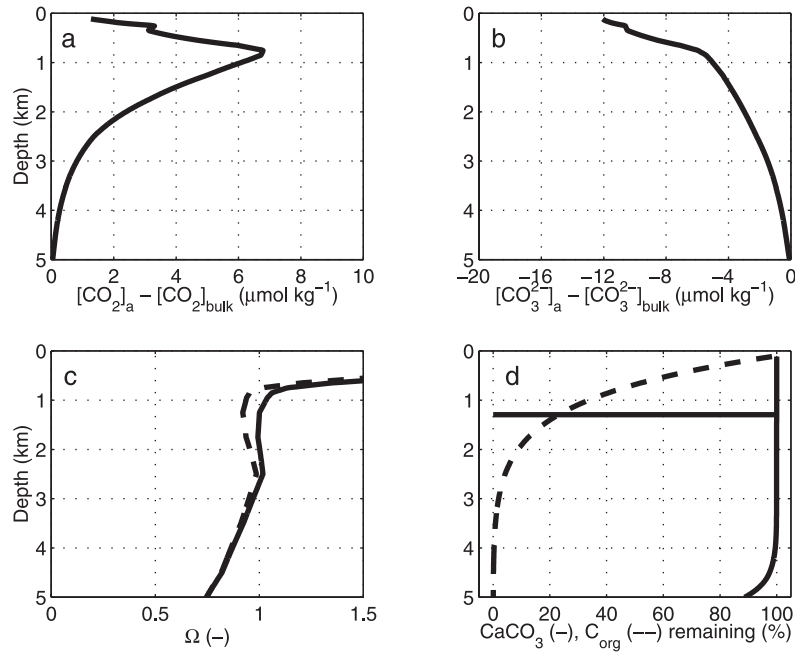


Figure 10. Respiration-driven dissolution in North Pacific considering aggregate of 0.15 μg calcite (1,000 *E. huxleyi* cells) and initial organic carbon content of 15 μg C_{org}. (a) [CO₂] and (b) [CO₃²⁻] difference between aggregate surface and bulk sea water. (c) Calcite saturation (solid line, bulk value; dashed line, aggregate value). (d) C_{org} (dashed line) and CaCO₃ (solid line) remaining in aggregate. Depth of bulk saturation horizon at ~0.8 km is marked by a straight solid line.

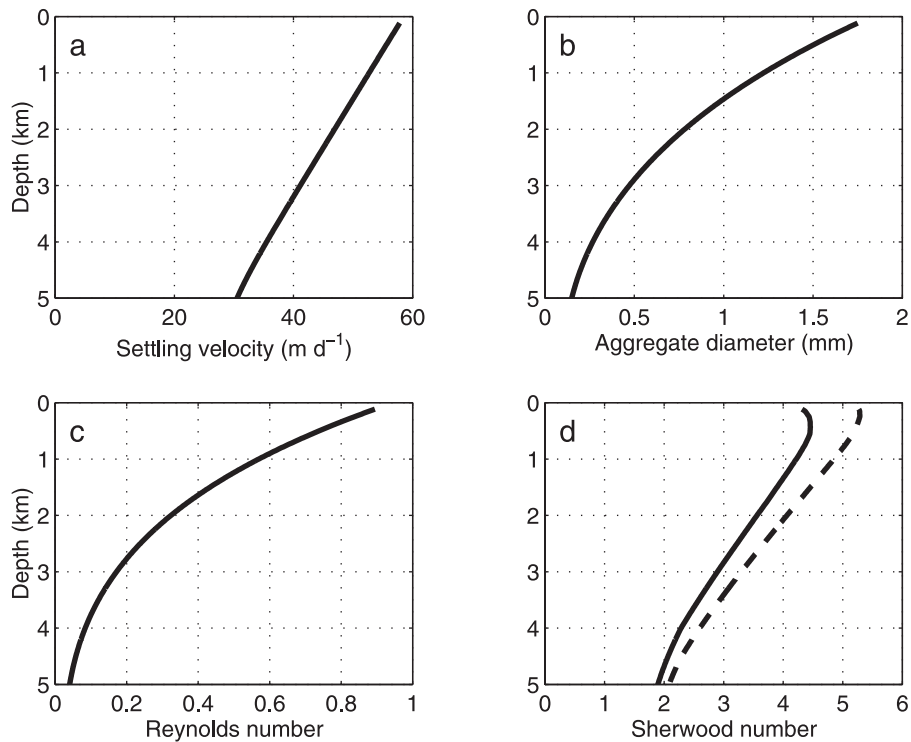


Figure 11. Respiration-driven dissolution in North Pacific considering aggregate of 0.15 μg calcite (1,000 *E. huxleyi* cells) and initial organic carbon content of 15 μg C_{org}. (a) Settling velocity, decreasing as aggregate gets smaller due to C_{org} remineralization. (b) Aggregate diameter. (c) Reynolds number. (d) Sherwood numbers (solid line, CO₂; dashed line, CO₃²⁻).

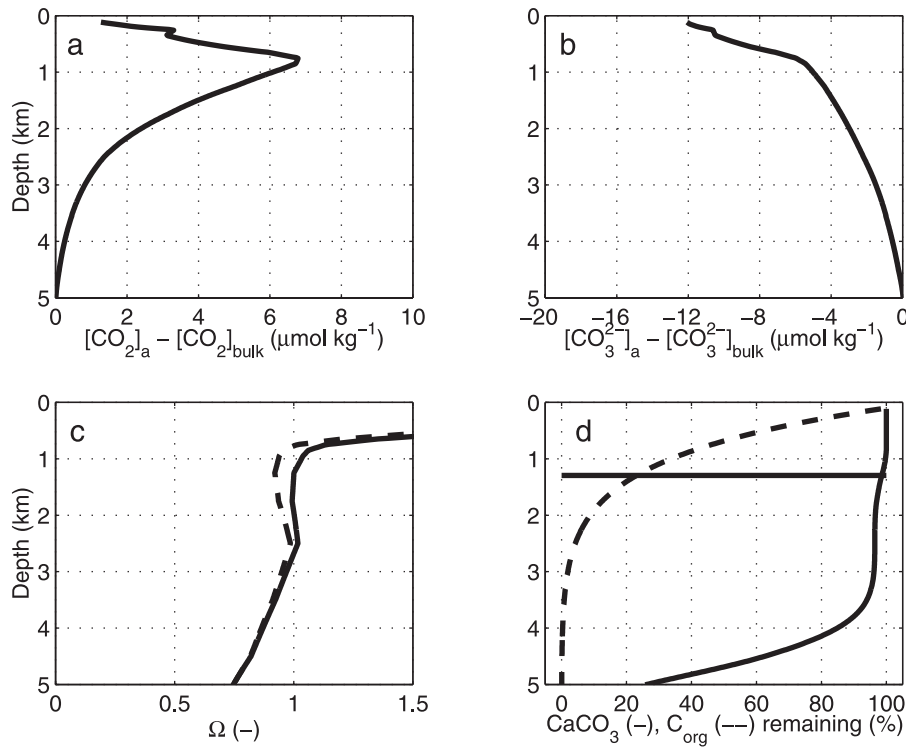


Figure 12. Respiration-driven dissolution in North Pacific, same as Figure 10, but with dissolution kinetic parameters set to $(\kappa = 5 \text{ d}^{-1}, \eta = 3)$.

[31] Table 6 displays results varying the amount of organic matter in the aggregate. Inclusion of organic carbon always enhances the amount of calcite dissolved. In case C, where $\kappa = 5 \text{ d}^{-1}$ and $\eta = 3$, the influence of respiration is visible. In the case of linear kinetics (case D) only, where $\kappa = 0.38, \text{ d}^{-1}$, and $\eta = 1$, calcite dissolution due to respiration processes is significant.

[32] Table 7 shows model results for the same model run as in Table 6, but with $2.5 \mu\text{g}$ calcite content. Note that with a given dissolution rate a certain fraction rather than a certain amount of the calcite present is dissolved over some time interval (compare equation (1)). In principal, when doubling the amount of calcite present, mass dissolution is expected to double, too. Only when the release of carbonate ions from dissolution significantly perturbs the carbonate

system toward a more saturated state is the amount of calcite present relevant for the fraction dissolving per time interval. Therefore incorporating more calcite into the aggregate should not lead to less dissolution fraction wise simply because there is more calcite present, but because more calcite should make the aggregate larger and should make it settle faster.

[33] However, the fraction dissolved at a depth of 3 km does not differ significantly from the model results displayed in Table 6. This is due to the fact that calcite, with its large density (2.7 g cm^{-3}), does not influence the radius and hence does not influence the settling velocity of the aggregate significantly. This might be a drawback of the model formulation. Nevertheless, other estimates on marine snow settling velocities (see Table A2) conform to the settling velocities calculated by the present model, though they are a bit higher, as most aggregates investigated are between 1 and 10 mm in diameter, and the aggregate sizes modeled

Table 6. Model Results Using Different Dissolution Kinetics^a

C_{org} ($\mu\text{g C}$)	Calcite Dissolved, %			
	A ($\kappa, \eta = (5, 4.5)$)	B ($\kappa, \eta = (1, 2.9)$)	C ($\kappa, \eta = (5, 3)$)	D ($\kappa, \eta = (0.38, 1)$)
0	0.0	0.0	0.0	9.0
1	0.0	0.0	0.1	17.7
2	0.0	0.0	0.2	23.2
5	0.0	0.2	0.6	35.5
10	0.0	0.5	1.9	48.8
15	0.1	1.0	3.8	57.5

^aDisplayed is fraction of calcite dissolved at 3 km depth (North Pacific), depending on organic carbon content. Sources are Keir [1980] for $(\kappa, \eta) = (5, 4.5)$, Walter [1985] for $(\kappa, \eta) = (1, 2.9)$, Morse [1978] for $(\kappa, \eta) = (5, 3)$, and Hales and Emerson [1997] for $(\kappa, \eta) = (0.38, 1)$.

Table 7. Model Results Using Different Dissolution Kinetics^a

C_{org} ($\mu\text{mol C}$)	Calcite Dissolved, %			
	A ($\kappa, \eta = (5, 4.5)$)	B ($\kappa, \eta = (1, 2.9)$)	C ($\kappa, \eta = (5, 3)$)	D ($\kappa, \eta = (0.38, 1)$)
0	0.0	0.0	0.0	5.8
1	0.0	0.0	0.1	12.5
2	0.0	0.0	0.1	18.2
5	0.0	0.1	0.5	31.5
10	0.0	0.5	1.8	46.3
15	0.1	1.0	3.7	55.8

^aSame model run as displayed in Table 6, but with $2.5 \mu\text{g}$ calcite.

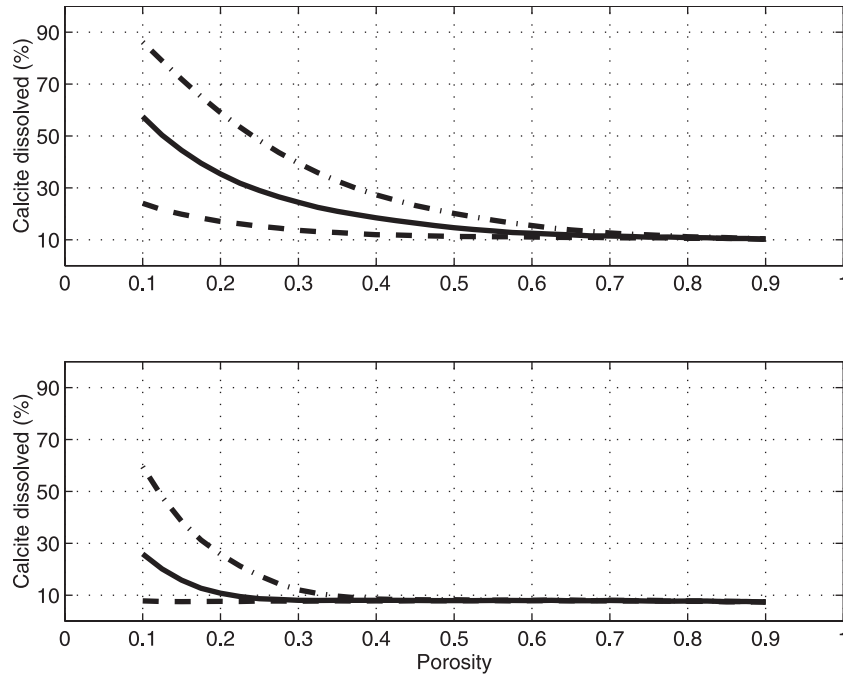


Figure 13. Dependency of respiration-driven dissolution at 3 km depth on porosity of aggregate for (top) North Pacific and (bottom) equatorial Pacific setting. Organic carbon content is $5 \mu\text{g C}$ (dashed line), $10 \mu\text{g C}$ (solid line), and $15 \mu\text{g C}$ (dash-dotted line).

here are on the lower end of this range. The marine snow particles investigated by *Allredge and Gotschalk* [1988] to derive the formulation (equation (9)) partly contained diatoms or fecal pellets, which are comparable in density to calcite.

[34] We now investigate what parameter variations would yield an aggregate that exhibits significant calcite dissolution. The main reason for the low effectiveness of respiration-driven dissolution is the porosity of the aggregate. High porosities lead to large diameters. Given a constant flux of, for example, CO_2 , the concentration gradient between the aggregate surface and the bulk medium decreases with increasing radius. Thus larger diameters at constant source strength Q are unfavorable for creating locally undersaturated chemical environments. To overcome these disadvantages with respect to calcite dissolution, the aggregate has to be loaded with large amounts of organic matter, which in turn increases the radius drastically due to the low density of C_{org} . This makes the aggregate settle faster, according to equation (9). The effect of a high settling velocity is twofold. It reduces the time the aggregate spends in undersaturation, and it decreases the thickness of the boundary layer, which in turn decreases the concentration gradient, as can be seen from equations (11)–(14).

[35] With small radius and resulting low settling velocity, the thickness of the diffusive boundary layer is approximately r_a , while it is $< r_a$ at large radius and high settling velocities due to the increase of the Sherwood number with increasing velocities. This promotes loss of respiratory CO_2 and thus less dissolution. Because of the high porosity of the aggregate and its resulting fractal geometry, the mass, i.e., organic carbon content, does not scale as r_a^3 , but in fact

only as $\sim r^{1.4}$, corresponding to the fractal dimension [Logan and Wilkinson, 1990; Allredge, 1998]. Thus the CO_2 source cannot keep up with the increasing surface (scaling as r_a^2) through which it diffuses when the aggregate gets larger. Thus, given the high porosity of the aggregate, an increase in size is unfavorable for respiration-driven dissolution because of increased settling velocity (i.e., less time spent in the water column), diminished thickness of the boundary layer (resulting in decreased concentration gradients), and a negative scaling ratio of respiratory CO_2 source to diffusion area.

[36] Because of the idealized geometry of the aggregate in the model, the organic carbon content in the model actually scales as r_a^3 . Nevertheless, respiration-driven dissolution correlates negatively with size, which means that the other two mechanisms outweigh the (in the model) positive scaling ratio of respiratory CO_2 source to diffusion area. Thus the model somewhat overestimates the potential of respiration-driven dissolution of CaCO_3 in marine snow aggregates.

[37] In order to quantify these relationships, the model is run with variable porosity. Results are illustrated in Figure 13. Respiration-driven dissolution is significant in the North Pacific provided $\phi \leq 0.4$ and is significant in the equatorial Pacific when $\phi \leq 0.2$. However, these results may be over estimations, since the settling velocity parameterization (equation (9)) has been derived with aggregate shaving porosity $\phi \geq 0.9$. Aggregates with smaller porosity are expected to settle faster, because the density increases with decreasing porosity. Stokes' law is not valid for the model's parameter range in Figure 13 since its application leads to Reynolds numbers > 1 .

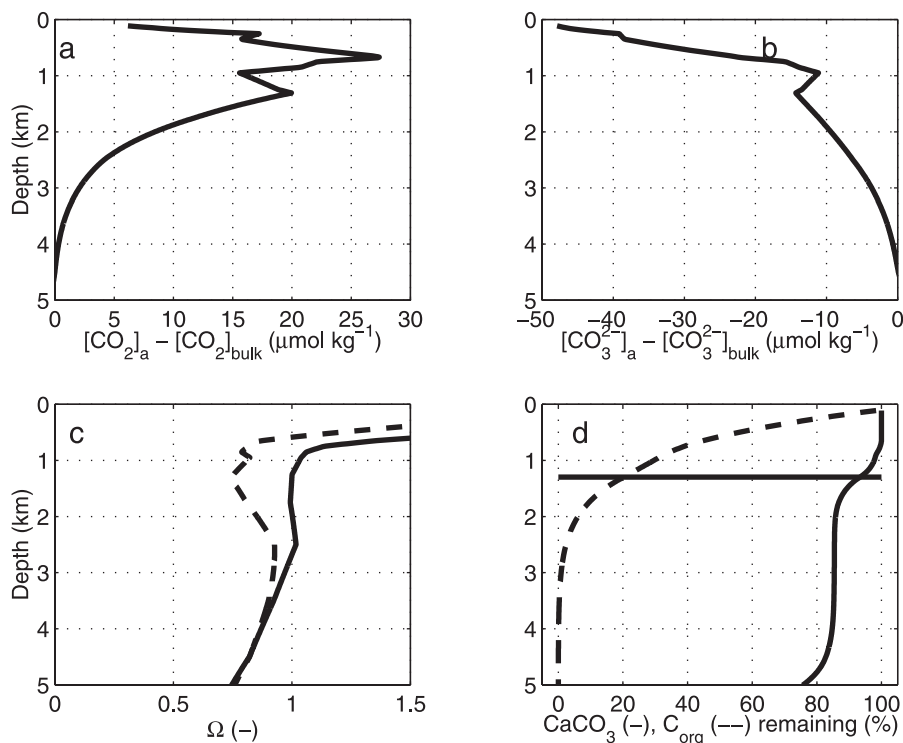


Figure 14. Respiration-driven dissolution in North Pacific, same as Figure 10, but with aggregate of $1 \mu\text{g}$ calcite and initial organic carbon content of $10 \mu\text{g C}$. Porosity is set to $\phi = 0.3$.

[38] A specific model run with $\phi = 0.3$ and $10 \mu\text{g C}$ organic carbon is shown in Figure 14. Between 1 and 2 km depth, 14% of the calcite content is dissolved due to organic matter respiration. Then the organic matter has vanished, and calcite dissolution ceases until, at ~ 4.5 km depth, bulk undersaturation is strong enough to trigger some more dissolution. The gradients in $[\text{CO}_2]$ and $[\text{CO}_3^{2-}]$ (Figures 14a and 14b) are much larger than with porosity 0.9 (compare Figure 10). The kink at 1 km is due to reduced organic matter remineralization as a consequence of oxygen deficiency, which is illustrated in Figure 15. Decreasing the porosity reduces the diffusive fluxes and the aggregate diameter, which enhances the oxygen concentration gradient. Oxygen deficiency appears with 5, 10, and $15 \mu\text{g C}_{\text{org}}$ when $\phi \leq 0.3, 0.5,$ and 0.625 , respectively.

4. Conclusions

[39] The derived physical constraints reveal that carbonate dissolution in the water column is feasible. As far as calcite is concerned, literature data yield that only coccolithophorids and coccoliths sink at rates that make dissolution in the water column possible. Foraminifera sink so fast that virtually no dissolution takes place before reaching the seafloor. On the other hand, the sinking rates given in Appendix A all apply to empty (senescent) foraminifera shells. Living organisms are likely to settle much slower (J. Bijma, personal communication, 1999). There is very limited work on pteropod settling rates; they are expected to sink at least as fast as foraminifera. Only because of the better solubility of aragonite compared to calcite, water

column dissolution of pteropods can be expected, ranging up to 90% in the model applied to the North Pacific at 5 km depth (Figures 8 and 9). Thus the alkalinity maximum in intermediate waters of the Pacific Ocean might be explained in part by water column dissolution of pteropods.

[40] Respiration-driven dissolution of calcite in the water column seems to be unlikely, considering the results of the model presented here. The size, settling velocity, and porosity of marine snow aggregates are unfavorable for creating a microenvironment with gradients sufficient to convert an oversaturated bulk environment into a locally undersaturated state. However, the amount of modeled calcite dissolution also depends on the kinetic parameters, which are still a subject of debate. The parameters proposed by Keir [1980] lead to slow dissolution kinetics, so the standard model runs presented here give a conservative view. Even with these slow dissolution kinetics, significant respiration-driven dissolution is calculated for porosities of < 0.4 . There is no evidence in the literature for marine snow aggregates having porosities smaller than 0.9. However, small aggregates may well exhibit decreased porosities [Ploug *et al.*, 1999a, 1999b]. The porosity of marine snow aggregates increases with increasing aggregate size, because they are fractal objects, with fractal dimensions of ~ 1.4 – 1.5 [Logan and Wilkinson, 1990; Alldredge, 1998]. Thus small and less porous aggregates, which are more favorable for respiration-driven dissolution, cannot be ruled out. The model may be improved by adopting a less idealized geometry. The heterogeneous nature of marine snow aggregates may lead to chemical environments inside the aggregate that are not homogeneous as modeled here, altering

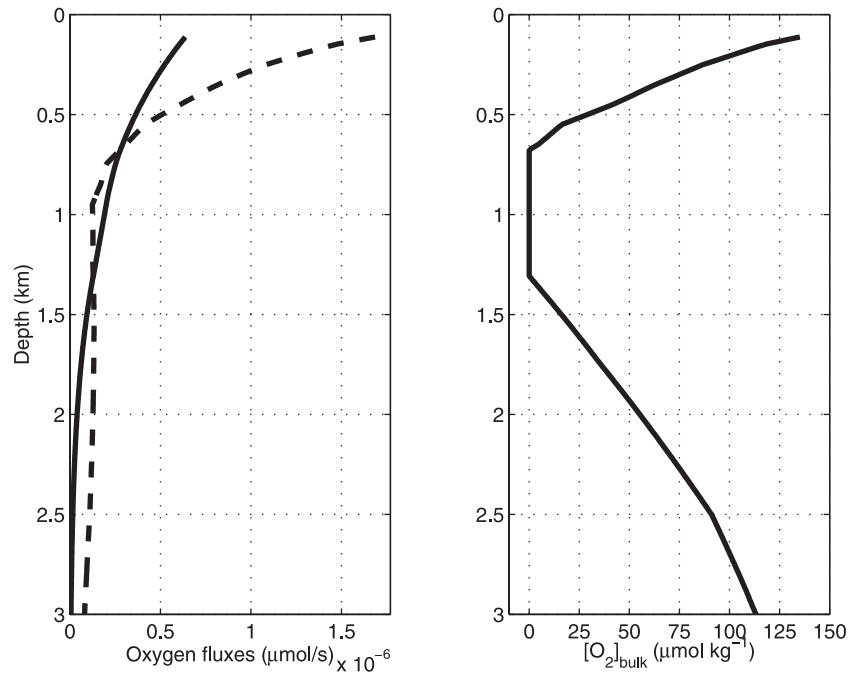


Figure 15. (left) Oxygen remineralization flux (solid line) and maximal flux possible (dashed line) to prevent oxygen deficiency. At ~ 1 km depth the remineralization flux is reduced. (right) Oxygen concentration at aggregate surface.

shape and magnitude of the microenvironment around the aggregate.

[41] Summing up, the postulated dissolution of calcium carbonate in the water column [Milliman *et al.*, 1999] cannot be explained by the mechanisms tested here. Thus, provided that the estimates by Milliman *et al.* [1999] are correct, other processes have to be investigated. For example, single coccoliths may end up as suspended particles, extending their presence in the water column considerably. If $[\text{CO}_3^{2-}]$ is such that undersaturation is evident, they are then certainly subject to dissolution. However, most single coccoliths may be scavenged by aggregates before they reach depths where undersaturation prevails [Stolzenbach, 1993; Jackson and Burd, 1998; Sherrell *et al.*, 1998]. To the authors' knowledge, no estimates exist on the fraction of single coccoliths reaching those depths. Thus the contribution of this specific mechanism to calcite water column dissolution remains open. Yet another dissolution mechanism may be attributed to dissolution in zooplankton guts, which, in a model study, has been shown to contribute significantly to calcium carbonate water column dissolution [Jansen and Wolf-Gladrow, 2001].

Appendix A: Settling Velocities

[42] Young [1994] states that single coccolithophorid cells are small enough to settle according to laminar flow, as may be formalized in the Stokes equation. For spherical particles of 4–20 μm diameter, he calculates sinking velocities of 1–10 m d^{-1} . Alldredge and Gotschalk [1988] observed settling velocities of large aggregates (diameters from 2.4 to 75 mm) in the range of 35–113 m d^{-1} . For solitary

coccolithophorids, Smayda [1971] finds settling velocities ranging from 0.25 to 10 m d^{-1} . Thus, depending on the location of the seafloor relative to the calcite saturation horizon, solitary coccolithophorids have a fair chance to dissolve in the water column (compare section 1). Honjo and Roman [1978] remark that coccolithophorids often sink rapidly to great depths enclosed in fecal pellets, then, after being expelled from the pellet, reduce to settling speeds ranging from 0.15 to 1.3 m d^{-1} and dissolve quickly. A typical pellet contains $\sim 10^5$ coccoliths [Honjo, 1976].

[43] Settling velocities of foraminifera have been investigated by a number of authors [Berger and Piper, 1972; Honjo, 1977; Bijma *et al.*, 1994; Fok-Pun and Komar, 1983]. Takahashi and Be [1984] state that sinking rates of spinose species are on average 3-fold slower than those of the nonspinose species. Furthermore, high settling velocities do not necessarily mean that particles are removed from surface waters fast, as Alldredge and Silver [1988] point out. Many aggregates may be kept in the mixed layer for weeks, accumulating at the thermocline. Literature data on pteropod sinking rates is very scarce. Details are given in Tables A1 and A2.

Appendix B: Carbonate Dissolution Kinetics

[44] The dissolution rate of calcite or aragonite may be described as $R = \kappa (1 - \Omega)^\eta$, where $\Omega = [\text{CO}_3^{2-}]_{\text{insitu}} / [\text{CO}_3^{2-}]_c$ is the saturation with respect to calcite or aragonite, calculated as the quotient of in situ carbonate concentration and critical carbonate concentration, κ (d^{-1}) is the rate constant, and η the order of the reaction [Keir, 1980; Walter and Morse, 1985]. An alternative rate equation for aragonite

Table A1. Settling Velocities of Single Cells of Different Carbonate Producers

Species	Settling Velocity, m d ⁻¹	Reference	Vital Status
<i>Coccolithophorids</i>			
<i>Coccolithus huxleyi</i>	1.5	<i>Smayda</i> [1971]	living cells
<i>Cricosphaera elongata</i>	0.25	<i>Smayda</i> [1971]	living cells
<i>Cyclococcolithus fragelisi</i>	10	<i>Smayda</i> [1971]	living cells
<i>Cyclococcolithus fragelisi</i>	>100	<i>Smayda</i> [1971]	senescent, in aggregates
<i>E. huxleyi</i>	0.15	<i>Honjo</i> [1977]	not specified
<i>Coccolithus neohelis</i>	0.16	<i>Honjo</i> [1977]	not specified
<i>Coccolithus leptopora</i>	1.3	<i>Honjo</i> [1977]	not specified
Maximal range	0.15–>100		
<i>Foraminifera</i>			
<i>Globorotalia hirsuta</i>	1275–1925	<i>Fok-Pun and Komar</i> [1983]	senescent
<i>Globigerinoides ruber</i>	415–1295	<i>Fok-Pun and Komar</i> [1983]	senescent
<i>Globigerinoides sacculifer</i>	775–2075	<i>Fok-Pun and Komar</i> [1983]	senescent
<i>Globigerinoides sacculifer</i>	500–2250	<i>Bijma et al.</i> [1994]	senescent
<i>Orbulina universa</i>	2140–3440	<i>Fok-Pun and Komar</i> [1983]	senescent
Not specified	170–1300	<i>Honjo</i> [1977]	not specified
Various species	260–2000	<i>Berger and Piper</i> [1972]	senescent
Various spinose species	4–2350	<i>Takahashi and Be</i> [1984]	not specified
Various nonspinose species	100–2820	<i>Takahashi and Be</i> [1984]	not specified
Maximal range	40–3440		
<i>Pteropods</i>			
Aggregates of <i>Limacina retroversa</i>	80–1080	<i>Noji et al.</i> [1997]	not specified

dissolution is given by $R = \kappa ([\text{CO}_3^{2-}]_c - [\text{CO}_3^{2-}]_{\text{insitu}})^n$ [Acker et al., 1987]. The dissolution rate constant is usually attributed to specific properties of the particle, such as geometry and particle size of the calcium carbonate in question [Keir, 1980]. The order of the reaction is thought to reflect the pure kinetics of the chemical reaction and thus should be universal.

[45] The rate order of calcite dissolution kinetics is not well constrained, as values cited in the literature range from 1 [Hales and Emerson, 1997] to >5 [Keir, 1980]. The latter finds a value of 4.5 ± 0.7 in dissolution experiments with a wide range of species as well as with mixed sediment probes. Hales and Emerson [1997] fit $\eta = 1$ to data obtained from in situ pore water measurements. Svensson and Dreybrodt [1992] find the rate order to be dependent on the distance from equilibrium. For saturation values of <0.8 , they measure a rate order of 1.5–2.2, whereas the dissolution slows down to a rate order of 4 when the medium is closer to equilibrium. Burton et al. [1951], considering the precipitation of calcite, calculate from theory a rate order that changes with distance from equilibrium. Dreybrodt [1988] states that precipitation and dissolution principally may be described by the same

equation type. The kinetics of aragonite dissolution are not as thoroughly investigated. However, it is generally assumed that the rate order of aragonite dissolution is a little less than that of calcite dissolution; that is, when undersaturation is the same, aragonite dissolves more quickly [Keir, 1980; Morse and Berner, 1979].

[46] Dissolution kinetics are influenced by a number of inhibitors, such as organic matter, the contribution of Mg calcite, or the presence of phosphate [Morse, 1974b; Walter and Hanor, 1979]. Varying $[\text{PO}_4^{3-}]$ from 0.1 to 10 mmol kg⁻¹, Morse and Berner [1979] find that the rate order increases from 3 to 17.

[47] Morse [1974a] has introduced the so-called pH-stat technique to study dissolution kinetics of CaCO₃, where the degree of undersaturation during an experimental run is kept fixed by adding acid or base to maintain a constant pH. Earlier work by other researchers adopts the free-drift technique, in which the system is started at undersaturation and allowed to react toward equilibrium. Morse and Berner [1979] state an accuracy in determination of the dissolution rate of $\pm 2\%$ for the pH-stat technique. The free-drift technique is generally considered to be less accurate, especially

Table A2. Settling Velocities of Biogenic Aggregates

Particle Type	Settling Velocity, m d ⁻¹	Reference
Marine snow aggregates	1–280	<i>Diercks and Asper</i> [1997]
Marine snow aggregates	1–368	<i>Allredge and Silver</i> [1988]
Marine snow aggregates	43–95	<i>Shanks and Trent</i> [1980]
Aggregates of phytoplankton detritus	100–150	<i>Lampitt</i> [1985]
Miscellaneous particles	67–131	<i>Lorenzen et al.</i> [1983]
Miscellaneous particles (equatorial Pacific)	>180	<i>Honjo et al.</i> [1995]
Miscellaneous particles (North Atlantic)	70	<i>Honjo et al.</i> [1995]
Miscellaneous particles (equatorial Pacific)	80–270	<i>Berelson</i> [2002]
Miscellaneous particles (Arabian Sea)	90–330	<i>Berelson</i> [2002]

near equilibrium [Morse, 1983]. Sjöberg and Rickard [1983] have employed both techniques to obtain insight into the influence of experimental design on the measured rates. They observe that the stirring rate, ω (revolutions per second), is an important parameter, as the dissolution rate behaves like $R \propto \omega^u$, where u is the stirring coefficient, which they find, for crystals at pH 8.3, to range between 0.63 and 0.85. In this context it is important to note that some experimental work has been done without significantly stirring the medium. Keir [1980], for example, merely excites the medium to maintain the particles in suspension. Hence any microenvironment that is created during the dissolution process and that is higher saturated than the bulk water due to the increase of CO₃²⁻ concentration is not destroyed by advection, and thus dissolution rates are likely to be underestimated, leading to an overestimation of the rate order.

[48] **Acknowledgments.** We thank Jelle Bijma, Michael Rutgers van der Loeff, and Ulf Riebesell for valuable discussions. Comments by David Archer and one anonymous reviewer improved the manuscript.

References

- Acker, J. G., R. H. Byrne, S. Ben-Yakoov, R. A. Feely, and P. R. Betzer, The effect of pressure on aragonite dissolution rates in seawater, *Geochim. Cosmochim. Acta*, 51, 2171–2175, 1987.
- Allredge, A. L., Discarded appendicularian houses as sources of food, surface habitats, and particulate organic matter in planktonic environments, *Limnol. Oceanogr.*, 21(1), 14–23, 1976.
- Allredge, A. L., The chemical composition of macroscopic aggregates in two neritic seas, *Limnol. Oceanogr.*, 24(5), 855–866, 1979.
- Allredge, A., The carbon, nitrogen and mass content of marine snow as a function of aggregate size, *Deep Sea Res., Part I*, 45, 529–541, 1998.
- Allredge, A. L., and Y. Cohen, Can microscale chemical patches persist in the sea? Microelectrode study of marine snow, fecal pellets, *Science*, 235, 689–691, 1987.
- Allredge, A. L., and C. Gotschalk, In situ settling behavior of marine snow, *Limnol. Oceanogr.*, 33(3), 339–351, 1988.
- Allredge, A. L., and C. C. Gotschalk, Direct observations of the mass flocculation of diatom blooms: Characteristics, settling velocities and formation of diatom aggregates, *Deep Sea Res.*, 36, 159–171, 1989.
- Allredge, A. L., and M. W. Silver, Characteristics, dynamics and significance of marine snow, *Prog. Oceanogr.*, 20, 41–82, 1988.
- Anderson, L. A., and J. L. Sarmiento, Redfield ratios of remineralization determined by nutrient data analysis, *Global Biogeochem. Cycles*, 8(1), 65–80, 1994.
- Archer, D., A data-driven model of the global calcite lysocline, *Global Biogeochem. Cycles*, 10(3), 511–526, 1996.
- Archer, D., and E. Maier-Reimer, Effect of deep-sea sedimentary calcite preservation on atmospheric CO₂ concentration, *Nature*, 367, 260–263, 1994.
- Balch, W. M., P. M. Holligan, S. G. Ackleson, and K. J. Voss, Biological and optical properties of mesoscale coccolithophore blooms in the Gulf of Maine, *Limnol. Oceanogr.*, 36(4), 629–643, 1991.
- Beers, J. R., J. D. Trent, F. M. H. Reid, and A. L. Shanks, Macroaggregates and their phytoplanktonic components in the Southern California Bight, *J. Plankton Res.*, 8, 475–487, 1986.
- Berelson, W. M., Particle settling rates increase with depth in the ocean, *Deep Sea Res., Part II*, 49, 237–251, 2002.
- Berger, W. H., and D. J. W. Piper, Planktonic foraminifera: Differential settling, dissolution, and redeposition, *Limnol. Oceanogr.*, 17(2), 275–287, 1972.
- Bijma, J., C. Hemleben, and K. Wellnitz, Lunar-influenced carbonate flux of the planktic foraminifer Globigerinoides sacculifer (Brady) from the central Red Sea, *Deep Sea Res., Part I*, 41(3), 511–530, 1994.
- Broecker, W. S., and T. Takahashi, The relationship between lysocline depth and in situ carbonate ion concentration, *Deep Sea Res.*, 25, 65–95, 1978.
- Burton, W. K., N. Cabrera, and F. C. Frank, The growth of crystals and the equilibrium structure of their surfaces, *Philos. Trans. R. Soc. London, Ser. A*, 243(866), 299–348, 1951.
- Byrne, R. H., J. G. Acker, P. R. Betzer, R. A. Feely, and M. H. Cates, Water column dissolution of aragonite in the Pacific Ocean, *Nature*, 312, 321–326, 1984.
- Culberson, C., and R. M. Pytkowicz, Effect of pressure on carbonic acid, boric acid, and the pH in seawater, *Limnol. Oceanogr.*, 13(3), 403–417, 1968.
- Department of Energy, Handbook of methods for the analysis of the various parameters of the carbon dioxide system in sea water, version 2, edited by A. G. Dickson, and C. Goyet, *ORNL/CDIAC-74*, Carbon Dioxide Inf. and Anal. Cent., Oak Ridge, Tenn., 1994. (Available at <http://www-mpl.ucsd.edu/people/adickson>)
- Diercks, A.-R., and V. L. Asper, In situ settling speeds of marine snow aggregates below the mixed layer: Black Sea and Gulf of Mexico, *Deep Sea Res., Part II*, 44, 385–398, 1997.
- Dreybrodt, W., *Processes in Karst Systems: Physics, Chemistry, and Geology*, Springer-Verlag, New York, 1988.
- Emerson, S., and M. Bender, Carbon fluxes at the sediment-water interface of the deep-sea: Calcium carbonate preservation, *J. Mar. Res.*, 39(1), 139–162, 1981.
- Fernández, E., P. Boyd, P. M. Holligan, and D. S. Harbour, Production of organic and inorganic carbon within a large-scale coccolithophore bloom in the northeast Atlantic Ocean, *Mar. Ecol. Prog. Ser.*, 97, 271–285, 1993.
- Fiadeiro, M., The alkalinity of the deep Pacific, *Earth Planet. Sci. Lett.*, 49, 499–505, 1980.
- Fok-Pun, L., and P. D. Komar, Settling velocities of planktonic foraminifera: Density variations and shape effects, *J. Foraminiferal Res.*, 13(1), 60–68, 1983.
- Hales, B., and S. Emerson, Evidence in support of first-order dissolution kinetics of calcite in seawater, *Earth Planet. Sci. Lett.*, 148, 317–327, 1997.
- Hebel, D. V. W., Concentration and flux of trace metals, carbon-nitrogen, and particulate matter in marine snow, Master's thesis, San Francisco State Univ., San Francisco, Calif., 1983.
- Honjo, S., Coccoliths: Production, transportation and sedimentation, *Mar. Micropaleont.*, 1, 65–79, 1976.
- Honjo, S., Biogenic carbonate particles in the Ocean: Do they dissolve in the water column?, in *Marine Science*, vol. 6, *The Fate of Fossil Fuel CO₂ in the Oceans*, edited by N. R. Anderson and A. Malankoff, pp. 269–294, Plenum, New York, 1977.
- Honjo, S., and M. R. Roman, Marine copepod faecal pellets: Production, preservation and sedimentation, *J. Mar. Res.*, 36(1), 45–57, 1978.
- Honjo, S., J. Dymond, R. Collier, and S. J. Manganini, Export production of particles to the interior of the equatorial Pacific Ocean during the 1992 EqPac experiment, *Deep Sea Res., Part II*, 42, 831–870, 1995.
- Jackson, G. A., and A. B. Burd, Aggregation in the Marine Environment, *Environ. Sci. Technol.*, 32(19), 2805–2814, 1998.
- Jansen, H., and D. A. Wolf-Gladrow, Carbonate dissolution in copepod guts: A numerical model, *Mar. Ecol. Prog. Ser.*, 221, 199–207, 2001.
- Karp-Boss, L., E. Boss, and P. A. Jumars, Nutrient fluxes to planktonic osmotrophs in the presence of fluid motion, *Oceanogr. Mar. Biol. Ann. Rev.*, 34, 71–107, 1996.
- Keir, R. S., The dissolution kinetics of biogenic calcium carbonates in seawater, *Geochim. Cosmochim. Acta*, 44, 241–252, 1980.
- Lampitt, R. S., Evidence for the seasonal deposition of detritus to the deep-sea floor and its subsequent resuspension, *Deep Sea Res.*, 32, 885–897, 1985.
- Logan, B. E., and D. B. Wilkinson, Fractal geometry of marine snow and other biological aggregates, *Limnol. Oceanogr.*, 35, 130–136, 1990.
- Lorenzen, C. J., N. A. Welschmeyer, A. E. Copping, and M. Vernet, Sinking rates of organic particles, *Limnol. Oceanogr.*, 28(4), 766–769, 1983.
- Millero, F. J., Thermodynamics of the carbon dioxide system in the oceans, *Geochim. Cosmochim. Acta*, 59, 661–677, 1995.
- Milliman, J. D., P. J. Troy, W. M. Balch, A. K. Adams, Y.-H. Li, and F. T. Mackenzie, Biologically mediated dissolution of calcium carbonate above the chemical lysocline?, *Deep Sea Res., Part I*, 46, 1653–1669, 1999.
- Morse, J. W., Dissolution kinetics of calcium carbonate in sea water, III, A new method for the study of carbonate reaction kinetics, *Am. J. Sci.*, 274, 97–107, 1974a.
- Morse, J. W., Dissolution kinetics of calcium carbonate in sea water, V, Effects of natural inhibitors and the position of the chemical lysocline, *Am. J. Sci.*, 274, 638–647, 1974b.
- Morse, J. W., Dissolution kinetics of calcium carbonate in sea water, VI, The near-equilibrium dissolution kinetics of calcium carbonate-rich deep sea sediments, *Am. J. Sci.*, 278, 344–353, 1978.
- Morse, J. W., The kinetics of calcium carbonate dissolution and precipitation, in *Reviews in Mineralogy*, vol. II, *Carbonates: Mineralogy and*

- Chemistry*, edited by R. J. Reeder, pp. 227–264, Mineral. Soc. of Am., Washington, D. C., 1983.
- Morse, J. W., and R. C. Berner, Chemistry of calcium carbonate in the deep oceans, in *Chemical Modeling in Aqueous Systems*, vol. 93, ACS Symp. Ser., edited by E. A. Jenne, pp. 499–535, Am. Chem. Soc., Washington, D. C., 1979.
- Morse, J. W., J. De Kanel, and K. Harris, Dissolution kinetics of calcium carbonate in sea water, VII, The dissolution kinetics of synthetic aragonite and pteropod tests, *Am. J. Sci.*, 279, 488–502, 1979.
- Noji, T. T., U. V. Bathmann, B. von Bodungen, M. Voss, A. Antia, M. Krumholz, B. Klein, I. Peeken, C. I.-M. Noji, and F. Rey, Clearance of picoplankton-sized particles and formation of rapidly sinking aggregates by the pteropod, *Limacina retroversa*, *J. Plankton Res.*, 19, 863–875, 1997.
- Ploug, H., H.-P. Grossart, F. Azam, and B. B. Jørgensen, Photosynthesis, respiration, and carbon turnover in sinking marine snow from surface waters of Southern California Bight: Implications for the carbon cycle in the ocean, *Mar. Ecol. Prog. Ser.*, 179, 1–11, 1999a.
- Ploug, H., W. Stolte, and B. B. Jørgensen, Diffusive boundary layers of the colony-forming plankton alga *Phaeocystis* sp.—Implications for nutrient uptake and cellular growth, *Limnol. Oceanogr.*, 44(8), 1959–1967, 1999b.
- Pond, S., R. M. Pytkowicz, and J. E. Hawley, Particle dissolution during settling in the oceans, *Deep Sea Res.*, 18, 1135–1139, 1971.
- Prézelin, B. B., and A. L. Alldredge, Primary production of marine snow during and after an upwelling event, *Limnol. Oceanogr.*, 28(6), 1156–1167, 1983.
- Shanks, A. L., and J. D. Trent, Marine snow: Sinking rates and potential role in vertical flux, *Deep Sea Res. Part A*, 27, 137–143, 1980.
- Sherrell, R. M., M. P. Field, and Y. Gao, Temporal variability of suspended mass and composition in the Northeast Pacific water column: Relationships to sinking flux and lateral advection, *Deep Sea Res., Part II*, 45, 733–761, 1998.
- Sherwood, T. K., R. L. Pigford, and C. R. Wilke, *Mass Transfer*, McGraw-Hill, New York, 1975.
- Sjöberg, E. L., and D. Rickard, The influence of experimental design on the rate of calcite dissolution, *Geochim. Cosmochim. Acta*, 47, 2281–2285, 1983.
- Smayda, T. J., Normal and accelerated sinking of phytoplankton in the sea, *Mar. Geol.*, 11, 105–122, 1971.
- Stolzenbach, K. D., Scavenging of small particles by fast-sinking porous aggregates, *Deep Sea Res., Part I*, 40, 359–369, 1993.
- Svensson, U., and W. Dreybrodt, Dissolution kinetics of natural calcite minerals in CO₂-water systems approaching calcite equilibrium, *Chem. Geol.*, 100, 129–145, 1992.
- Takahashi, K., and A. W. H. Be, Planktonic foraminifera: Factors controlling sinking speeds, *Deep Sea Res.*, 31, 1477–1500, 1984.
- Takahashi, T., W. S. Broecker, and A. E. Bainbridge, Supplement to the alkalinity and total carbon dioxide concentration in the world oceans, in *Carbon Cycle Modelling*, vol. 16, *SCOPE Rep. Ser.*, edited by B. Bolin, pp. 159–199, John Wiley, New York, 1981.
- Trent, J. D., A study of macroaggregates in the Marine Environment, Ph.D. thesis, Scripps Inst. of Oceanogr., Univ. of Calif., San Diego, San Diego, 1985.
- Tyrrell, T., and A. H. Taylor, A modelling study of *Emiliania huxleyi* in the NE Atlantic, *J. Mar. Syst.*, 9, 83–112, 1996.
- Walsh, I., J. Dymond, and R. Collier, Rates of recycling of biogenic components of settling particles in the ocean derived from sediment trap experiments, *Deep Sea Res.*, 35, 43–58, 1988.
- Walter, L. M., and J. S. Hanor, Effect of orthophosphate on the dissolution kinetics of biogenic magnesian calcite, *Geochim. Cosmochim. Acta*, 43, 1377–1385, 1979.
- Walter, L. M., and J. W. Morse, The dissolution kinetics of shallow marine carbonates in seawater: A laboratory study, *Geochim. Cosmochim. Acta*, 49, 1503–1513, 1985.
- Westrich, J. T., and R. A. Berner, The role of sedimentary organic matter in bacterial sulfate reduction: The *G* model tested, *Limnol. Oceanogr.*, 29(2), 236–249, 1984.
- Young, J. R., Functions of coccoliths, in *Coccolithophores*, edited by A. Winter, pp. 63–82, Cambridge Univ. Press, New York, 1994.

H. Jansen, Meteorologisches Institut der Universität Hamburg, Bundesstrasse 55, Hamburg, D-20146 Germany. (heiko.jansen@dkrz.de)

D. A. Wolf-Gladrow and R. E. Zeebe, Alfred Wegener Institute for Polar and Marine Research, P.O. Box 12 01 61, D-27515 Bremerhaven, Germany. (dwolf@awi-bremerhaven.de; rzeebe@awi-bremerhaven.de)